

# Integrated quantum cascade laser-modulator using vertically coupled cavities

J. Teissier,<sup>1</sup> S. Laurent,<sup>1,a)</sup> C. Sirtori,<sup>1</sup> H. Debrégeas-Sillard,<sup>2</sup> F. Lelarge,<sup>2</sup> F. Brillouet,<sup>2</sup> and R. Colombelli<sup>3</sup>

<sup>1</sup>Laboratoire de Matériaux et Phénomènes Quantiques, Université Paris VII, CNRS UMR 7162-75205, Paris Cedex 13, France

<sup>2</sup>Alcatel-Thales III-V Laboratory, Alcatel Lucent Bell Laboratories, and Thales Research and Technology, 91460 Marcoussis, France

<sup>3</sup>Institut d'Electronique Fondamentale, Université Paris-Sud and CNRS, UMR8622, 91405 Orsay, France

(Received 18 March 2009; accepted 21 April 2009; published online 28 May 2009)

We demonstrated an integrated three terminal device able to modulate the cavity losses of quantum cascade lasers. By growing asymmetric doped quantum wells coupled to the laser's mode an absorption peak can be electrically shifted in and out the laser transition. The use of three terminals allows one to drive the laser independently from the wells and therefore to modulate the laser's amplitude with an electrical power of only a few milliwatts. This is far less than the power needed for a direct modulation of the laser light. © 2009 American Institute of Physics.

[DOI: 10.1063/1.3138779]

Progresses in the development of quantum cascade lasers (QCL) led recently to the demonstration of continuous wave operation at room temperature with Watt-level output powers.<sup>1</sup> This performance demonstrates that midinfrared QCLs are ideal devices for trace gas detection techniques<sup>2</sup> and can be an interesting candidate also for free space optical data communication.<sup>3</sup> These applications could benefit from the building of compact midinfrared emitting devices in which new functionalities are inserted, primarily the electrical control of the complex refractive index for amplitude and phase modulation purposes. These functionalities would be integrated in three terminal devices in order to control them independently from the laser driving current.

In this paper, we show that we can modulate the intensity of the laser by the electrical control of the imaginary part of the effective refractive index. This has been realized by exploiting the linear Stark effect of asymmetric coupled quantum wells (AQWs),<sup>4</sup> which allows one to electrically tune the peak absorption wavelength. The modulation of the laser intensity has been achieved up to now by direct modulation of the driving current.<sup>5</sup> To do so, however, a rather high modulation power around 100 mW is necessary. By electrically modulating the laser cavity optical losses, our approach allows to use a much lower voltage swing<sup>6</sup> and to separate the laser drive current from the amplitude modulation control. This technique applied to distributed feedback (DFB) lasers could avoid the linewidth enhancement observed for low frequency modulation and due to thermal effects.<sup>7</sup>

The top inset of Fig. 1 shows a schematic of the three terminal device studied in this paper. It is composed of two core sections: the laser active region and the AQW control region. These sections are separated by InP cladding layers and a highly doped GaInAs thin layer added to realize a third lateral terminal (see also Fig. 2). This lateral contact serves

as the ground contact and allows one to control independently the laser from the AQWs.

The active region consists of 35 periods of a four quantum well double phonon resonance design<sup>8</sup> grown on InP. The bottom inset of Fig. 1 represents the coupled quantum wells structure and the associated energy levels and wave functions of the control region. As can be seen on Fig. 1, the intersubband separation energy  $E_{12}$  between the first two levels of the structure is a linear function of the electric field applied to the wells. The shift is reproduced, with an excellent approximation, by the potential drop between the centers of the two wells. This linear Stark effect has already been extensively studied in Ref. 4. By tuning the absorption wavelength over the spectral range of the laser emission, we can therefore add controllable optical losses and modulate the laser intensity.

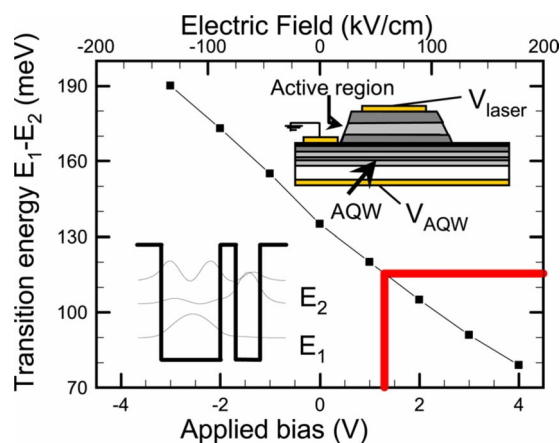


FIG. 1. (Color online) Intersubband transition energy  $E_{12}$  between the two first levels of AQW calculated as a function of the applied electric field (top horizontal axis). Bottom horizontal axis: corresponding voltage for a 2300 Å thick heterostructure. Insets: (top) schematic of a three terminal device, (bottom) conduction band (BC) profile of the AQW with the associated energy subbands and moduli squared of the wave functions. The wells are, respectively, 60 and 26 Å thick and separated by a 16 Å thick barrier.

<sup>a)</sup>Electronic mail: sabine.laurent@univ-paris-diderot.fr.

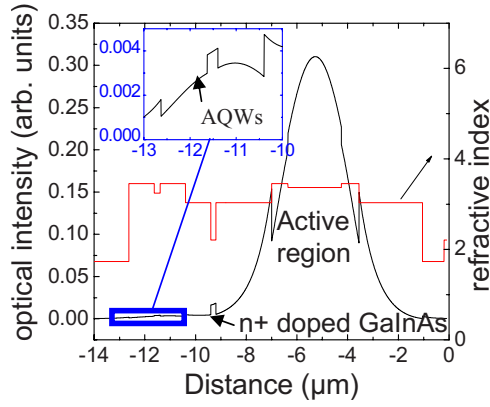


FIG. 2. (Color online) Mode profile (the moduli squared of the electric field is plotted) of the structure (left) and of the refractive index (right) as a function of the distance along the growth axis. Inset: close-up of the control region.

The design of the laser cavity must take into account two parameters: an efficient lateral extraction of the current passing through the active region and an optimized overlap of the laser mode over the AQW. To efficiently extract the current, we added above the control region a 1  $\mu\text{m}$  thick doped ( $1 \times 10^{17} \text{ cm}^{-3}$ ) InP layer followed by a highly doped ( $3 \times 10^{18} \text{ cm}^{-3}$ ) GaInAs layer of 200 nm, which ensures a good Ohmic contact. The overlap of the laser optical mode with the AQW region was chosen in order to add a few  $\text{cm}^{-1}$  to the optical losses, a value comparable with the gain of a quantum cascade laser.<sup>9</sup> To quantify the additional losses introduced by these AQWs, we calculate the absorption coefficient as<sup>10</sup>

$$\alpha_{\text{wells}}(\omega) = \frac{n_s e^2 \hbar}{2 \sqrt{\ln 2} \epsilon_0 c \eta m^* \gamma} f_{12} \times \exp\left[-\frac{(E_{12} - \hbar\omega)^2}{\gamma^2}\right] * \frac{\Gamma_{\text{wells}}}{L_{\text{wells}}}. \quad (1)$$

In this expression, we assume that  $\alpha_{\text{wells}}$  has a Gaussian line shape typical of a diagonal transition.<sup>11</sup> The constants  $e$ ,  $\hbar$ ,  $\epsilon_0$ , and  $c$  are, respectively, the electron charge, Planck's constant, vacuum dielectric constant, and speed of light;  $\eta$  is the effective refractive index,  $m^*$  is the effective mass,  $f_{12}$  and  $\sqrt{\ln 2} * \gamma$  are the oscillator strength and half width at half maximum of the transition.  $L_{\text{wells}}$  is the width of one period of the coupled quantum wells heterostructure and  $n_s$  is the sheet density.  $\Gamma_{\text{wells}}$  is the mode overlap factor with the control region.

By introducing in Eq. (1) the nominal values of  $n_s = 4.2 \cdot 10^{11} \text{ cm}^{-2}$ ,  $L_{\text{wells}} = 400 \text{ \AA}$ , and  $f_{12} = 0.4$ , we obtain a peak absorption coefficient,  $\alpha_{\text{wells}} \sim 700 \text{ cm}^{-1} \Gamma_{\text{wells}}$ . This value, typical for intersubband transition losses, imposes a small  $\Gamma_{\text{wells}}$  close to 0.1% to obtain  $\alpha_{\text{wells}}$  comparable to the gain coefficient at threshold ( $5\text{--}10 \text{ cm}^{-1}$ ).

The structure is optimized by first calculating the one dimensional optical mode and choosing the value of the overlap  $\Gamma_{\text{wells}}$ . The result of our simulation is represented on Fig. 2. The exact composition of the structure is given in Ref. 12. The model confirms that the cladding layers inserted between the control and active regions can be as thick as 3  $\mu\text{m}$  while still maintaining a sufficient overlap of the laser mode with the control region.

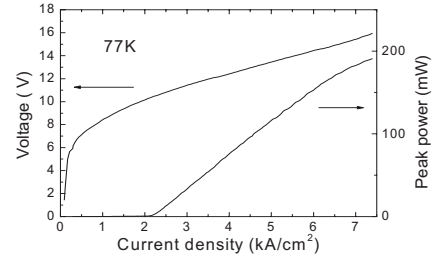


FIG. 3. Light current voltage characteristics of the electromodulator (no bias is applied on the wells region).

Two structures were grown by gas source molecular beam epitaxy. They are labeled in the following electro-modulator and reference. The reference has the same active region as the electromodulator, but the AQWs have been replaced by an InGaAs layer of the same thickness (doping  $n = 2 \times 10^{16} \text{ cm}^{-3}$ ). Each laser was soldered junction up on a copper submount.

For each sample, light-current-voltage characteristics were taken at 77 K in pulsed mode with a duty cycle of 0.05%. The current-voltage characteristic of the reference has been measured by applying the bias either between the top and lateral contacts, or between the top and back contacts. Both curves perfectly superimposed, meaning that the lateral contact does not add any significant series resistance.

Figure 3 shows the light-current-voltage curves for a 2.1 mm long and 29  $\mu\text{m}$  wide electromodulator. The measured threshold current is higher than for previous devices with similar active region<sup>8</sup> (2.2  $\text{kA/cm}^2$  instead of 1  $\text{kA/cm}^2$ ). This may be due to the  $n+$  doped GaInAs layer that increases the optical losses. However, recent experiments show that the GaInAs layer is not necessary, as the lateral contact can be directly taken on moderately doped InP layer without adding any significant Schottky contact.

To check the efficiency of the control region to modulate the light intensity, we measured the laser peak power  $P$  and the threshold current as a function of the bias applied to the AQWs,  $V_{\text{wells}}$ . The results are given in Fig. 4. We first notice that the dependence of both the laser power  $P$  and the threshold current  $J_{\text{th}}$  with the AQW bias reproduces the characteristic lineshape of an intersubband transition. This is expected as the AQW bias evolves linearly with the transition energy of the wells. The peak absorption is reached when the intersubband transition is at the same energy than the laser (see Fig. 1).

From Fig. 4(a), we can derive the relative absorption coefficient changes:  $\Delta\alpha/\alpha = \Delta J_{\text{th}}/J_{\text{th}} = 8\%$ . From this value, we can estimate  $\Gamma_{\text{wells}}$  between 0.1% and 0.2%, which is in good agreement with our design.<sup>13</sup> In Fig. 4(b), we plot the optical modulation depth  $\Delta P$  as a function of the bias on the control region  $V_{\text{wells}}$ . This is defined as  $P(V_{\text{wells}}) - P_{\text{max}}$ , where  $P(V_{\text{wells}})$  is the emitted power for different bias voltage on the AQW region and  $P_{\text{max}}$  is the highest measured power.  $\Delta P$  is  $\sim 12 \text{ mW}$  and constant with the injected current density, once the laser power is higher than the modulation depth ( $J \geq 2.4 \text{ kA/cm}^2$ ). The asymmetry observed in the modulation depth is due to an increase of the oscillator strength of the transition for high electric fields.<sup>14</sup> According to our calculations,  $f_{12}$  goes from 0.39 to 0.43 between  $V_{\text{wells}} = -2 \text{ V}$  and  $V_{\text{wells}} = 4 \text{ V}$ . As can be seen on Fig. 4(b),

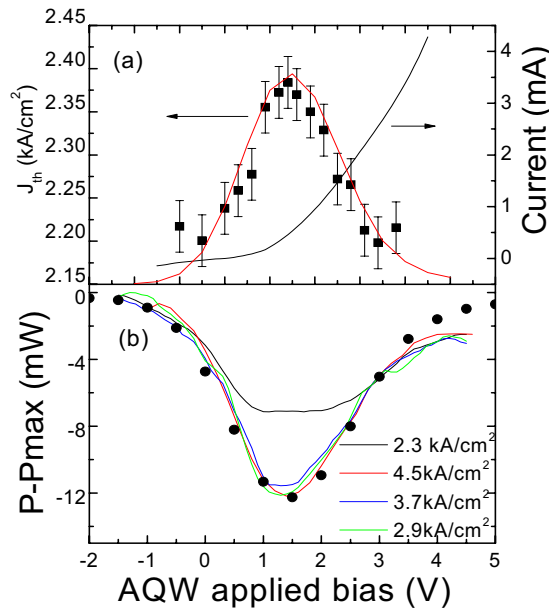


FIG. 4. (Color online) (a) Laser threshold current density (squares, left) and current passing through the wells (right) as a function of the CW bias applied to the wells. (b) Optical modulation depth,  $\Delta P$  for different current densities  $J$  injected in the laser (dots: fit). The data of  $\Delta P$  and  $J_{th}$  are fitted by the computed absorption lineshape,  $\alpha_{wells}$ .

our calculation of the absorption coefficient fits well the measurements.

Figure 4(a) shows also the current voltage characteristic of the control region, confirming that the electrical power used to modulate is of the order of 1 mW only. The asymmetry of this curve arises from an enhancement of the tunneling between the asymmetric quantum wells for positive bias.

The modulation speed of our system can be estimated by modeling the device by a  $RC$  parallel circuit, with  $R$  as the differential resistance and  $C$  as the capacitance of the control region.<sup>15</sup> By using the approach developed in Ref. 15,  $C$  can be estimated by a parallel plate approximation, and the resulting  $R_L C$  characteristic frequency of the circuit, estimated  $<100$  MHz since the surface contact of the control region was not optimized ( $\sim 250 \mu\text{m} \times 2.1 \text{mm}$ ), limits the frequency modulation of the system ( $R_L = 50 \Omega$  is the load resistance). Tens of gigahertz frequency response could be achieved by reducing the size of the control region. This could be realized by growing the AQWs at the top of the active region and by conceiving a multisection laser. Depending on the chosen architecture, the amount of modulated optical power could be optimized by a careful choice of the layers thicknesses, which determines the overlap between the laser mode and the AQW.

In conclusion, we demonstrated a three-terminal-device, where a control region is integrated within the cavity of a quantum cascade laser operating at  $\lambda \approx 10 \mu\text{m}$ . The control region allows modulation of the cavity losses and, as a consequence, of the laser output power. This system could avoid the linewidth enhancement observed by the direct modulation at low frequency and high duty cycle since a very small electrical power is needed to modulate.

We thank J.-R. Coudeville and A. Bousseksou for technical help and discussions. The device fabrication has been performed at the nanocenter CTU-IEF-Minerve, which is partially funded by the ‘‘Conseil General de l’Essonne.’’ We gratefully acknowledge financial support from the ‘‘Agence Nationale de la Recherche’’ (Project Metalguide No. 264).

<sup>1</sup>Y. Bai, S. Slivken, S. R. Darvish, and M. Razeghi, *Appl. Phys. Lett.* **93**, 021103 (2008).

<sup>2</sup>S. M. Cristescu, S. T. Persijn, S. T. E. L. Hekkert, and F. J. M. Harren, *Appl. Phys. B: Lasers Opt.* **92**, 343 (2008).

<sup>3</sup>F. Capasso, R. Paiella, R. Martini, R. Colombelli, C. Gmachl, T. L. Myers, M. S. Taubman, R. M. Williams, C. G. Bethea, K. Unterrainer, H. Y. Hwang, D. L. Sivco, A. Y. Cho, A. M. Sergent, H. C. Liu, and E. A. Whittaker, *IEEE J. Quantum Electron.* **38**, 511 (2002).

<sup>4</sup>F. Capasso, C. Sirtori, and A. Y. Cho, *IEEE J. Quantum Electron.* **30**, 1313 (1994).

<sup>5</sup>R. Paiella, F. Capasso, C. Gmachl, H. Y. Hwang, D. L. Sivco, A. L. Hutchinson, A. Y. Cho, and H. C. Liu *Appl. Phys. Lett.* **77**, 169 (2000).

<sup>6</sup>P. Holmstrom, P. Janes, U. Ekenberg, and L. Thylen, *Appl. Phys. Lett.* **93**, 191101 (2008).

<sup>7</sup>T. Aellen, R. Maulini, R. Terazzi, N. Hoyler, M. Giovannini, J. Faist, S. Blaser, and L. Hvozdar, *Appl. Phys. Lett.* **89**, 091121 (2006).

<sup>8</sup>C. Faugeras, S. Forget, E. B. Duchemin, H. Page, J. Y. Bengloan, O. Parillaud, M. Calligaro, C. Sirtori, M. Giovannini, and J. Faist, *IEEE J. Quantum Electron.* **41**, 1430 (2005).

<sup>9</sup>T. Gresch, R. Terazzi, J. Faist, and M. Giovannini, *Appl. Phys. Lett.* **94**, 031102 (2009).

<sup>10</sup>M. Helm, in *Intersubband Transitions in Quantum Wells: Physics and Device Applications I*, edited by H. C. Liu and F. Capasso (Academic, San Diego, CA, 2000), Vol. 62, pp. 1–99.

<sup>11</sup>K. L. Campman, H. Schmidt, A. Imamoglu, and A. C. Gossard, *Appl. Phys. Lett.* **69**, 2554 (1996).

<sup>12</sup>From top to buffer: GaInAs ( $3 \times 10^{18} \text{cm}^{-3}$ , 100 nm), InP ( $5 \times 10^{18} \text{cm}^{-3}$ , 0.85  $\mu\text{m}$ ), InP ( $1 \times 10^{17} \text{cm}^{-3}$ , 2.5  $\mu\text{m}$ ), GaInAs ( $2 \times 10^{16} \text{cm}^{-3}$ , 0.7  $\mu\text{m}$ ), active region, GaInAs ( $2 \times 10^{16} \text{cm}^{-3}$ , 0.64  $\mu\text{m}$ ), InP ( $1 \times 10^{17} \text{cm}^{-3}$ , 2.2  $\mu\text{m}$ ), GaInAs ( $3 \times 10^{18} \text{cm}^{-3}$ , 200 nm), InP ( $1 \times 10^{17} \text{cm}^{-3}$ , 1  $\mu\text{m}$ ), GaInAs ( $2 \times 10^{16} \text{cm}^{-3}$ , 1  $\mu\text{m}$ ), five periods of coupled QW separated by 300  $\text{Å}$  of AlInAs, GaInAs ( $2 \times 10^{16} \text{cm}^{-3}$ , 1  $\mu\text{m}$ ), InP ( $2 \times 10^{17} \text{cm}^{-3}$ , 2  $\mu\text{m}$ ), and buffer InP ( $5 \times 10^{18} \text{cm}^{-3}$ ).

<sup>13</sup>E. Benveniste, S. Laurent, A. Vasanelli, C. Manquest, C. Sirtori, F. Teulon, M. Carras, and X. Marcadet, *Appl. Phys. Lett.* **94**, 081110 (2009) (In the case of this paper, the mirror losses are  $\alpha_M \approx 6 \text{cm}^{-1}$  and the waveguide losses equal a few  $\text{cm}^{-1}$ ).

<sup>14</sup>J. Faist, C. Sirtori, F. Capasso, L. N. Pfeiffer, K. W. West, D. L. Sivco, and A. Y. Cho, in *Intersubband Transitions in Quantum Wells: Physics and Device Applications I*, edited by H. C. Liu and F. Capasso (Academic, San Diego, CA, 2000), Vol. 62, p. 109.

<sup>15</sup>H. C. Liu, J. Li, M. Buchanan, and Z. R. Wasilewski, *IEEE J. Quantum Electron.* **32**, 1024 (1996).